

Synthesized of Novel Imidazole-derived Schiff Base as a Corrosion Inhibitor of Carbon Steel in Acidic Medium Supported by Electrochemical and DFT Studies

S.S. Al-Najjar and A.Y. Al-Baitai*

Department of Chemistry, College of Science, Al-Nahrain University, Baghdad, Iraq

(Received 17 June 2021, Accepted 24 September 2021)

In this work, a newly synthesized imidazole derivative, namely (N,N'E,N,N'E)-N,N'-(thiophene-2,5-diylbis(methanylylidene))bis(1H-benzo[d]imidazol-2-amine) which is donated as (SJ1), was tested as an inhibitor in controlling the corrosion of carbon steel in 0.1 M hydrochloric acid solution by using open circuit potential (OCP), potentiodynamic polarization (PDP), at four different temperatures (293, 303, 313 and 323 K) and various of SJ1 concentrations. Furthermore, the surface morphology was investigated using both the Atomic force microscopy (AFM) and Scanning Electron Microscope (SEM), respectively. The effect of using different concentrations of SJ1 and temperature was also investigated. SJ1 was synthesized and characterized via using the UV-Vis, mass spectroscopy, ¹H NMR and ¹³C NMR spectroscopy, and the element analysis CHN. The experimental results shown that SJ1 can consider as an excellent corrosion inhibitor for carbon steel in 0.1 hydrochloric acid solution, by presence of SJ1 the corrosion of carbon steel was significantly suppressed. The inhibition efficiency is increased with increasing the inhibitor concentration but is decreased with the increases of temperature, and the optimum inhibition efficiency by 0.5 mM of SJ1 is 96%. The adsorption behavior of SJ1 onto the surface of the carbon steel in the acidic environment was investigated and found is obeyed the Langmuir adsorption isotherm. Also, both the thermodynamic and kinetic parameters are computed and discussed. The observed results of the free energy of adsorption ΔG_{ads} of $-38.12 \text{ kJ mol}^{-1}$ suggested that adsorption of SJ1 onto the surface of carbon steel has both types of interaction physisorption/chemisorption. The modeling methods were conducted by using the density functional theory (DFT/B3LYP) to study the electronic properties of SJ1 to discover the correlation between the molecular structure and the inhibitor efficiency. Both the experimental and simulation results were in good agreement with each other in this concern and authorize that SJ1 is an effective inhibitor.

Keywords: Carbon steel, Polarization method, DFT, SEM, AFM

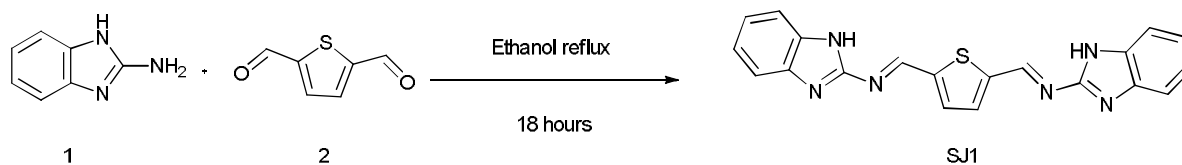
INTRODUCTION

Carbon steel is considered one of the most important industrial materials that is used as a raw manufactured by way of an alloy of iron, carbon, with some trace amounts of other metals [1-2]. Due to the excellent features of carbon steel as mechanical, welding, and annealing, and the availability of low cost [3] also carbon steel reveals excellent qualities that satisfy its application in different sectors such as in industry, oil, and gas [2, 4-6]. In many

industry fields are using acids as mineral acids or organic acids to cleaning and descaling of steel substrates or to dissolve the rubble, remove the mud to create channels through rocks to access the crude oil [7], and as a result of that the carbon steel employed for oil explorations in wells will be corroded due to the harsh effects of the acid solutions, which have been used as solvent to dissolve the rocks on the oil wells. This practice is accepted around the world to improve the production of extra oil and gas, and the method of using (5-28%) HCl is reported as the most prominent [2].

Today, due to the corrosion damages that effect on the main three fields: economics, safety, and conservation,

*Corresponding author. E-mail: dr_asmaabayati@yahoo.com



Scheme 1. Synthesis of SJ1

therefore, its became very important to control the corrosion damages by using different methods and techniques such as coating the surfaces or by adding some materials such as inorganic or organic compounds to play as corrosion inhibitors, and cathodic protection [8-11]. However, by considering the fact that mentioned by using the acidic as corrosive solutions for different purposes, the use of the inhibitor is consider one of the most effective methods that have been shown and improved the controlling on the corrosion process due to the easily practicable, efficient, and economically [12]. There are a huge number of different inorganic and organic compounds have been used as corrosion inhibitors for the carbon steel in acidic corrosive medium [13]. Control the corrosion damages by using the corrosion inhibitors depends on the chemical structure of the inhibitor which plays an important role in the adsorption mechanism of the inhibitor onto the surface of the metal/alloy to form a protective layer as film. Such organic molecules with the presence of heteroatoms which are included: oxygen, sulfur, and nitrogen, or with the π -electrons or those possessing certain functional groups such as $-\text{NH}_2$, $-\text{COOH}$, or $-\text{OH}$ (amines, acids, alcohols, phenols, amino acids, *etc.*) [13-14]. In addition, the other preferred organic inhibitors can include the drugs, amino acid, biopolymers, or ionic liquids and the heterocyclic organic compounds, such as triazoles, thiazoles, imidazoles benzimidazoles, benzotriazoles, purine, or adenine [14]. All these make these inhibitors can have a strong interaction with the metal and formed of an effective protection layer over the surface of the metal/alloy that prevent the direct contact with the corrosive medium, and for the protection of the carbon steel particularly in the presences of hydrochloric acid the organic inhibitors are the most common used.

Recently, there are a huge number of Schiff bases compounds were prepared and used as corrosion inhibitors [14]. These inhibitors usually become efficient through adsorption on the surface of metal/alloy and the adsorption

consists of the structure, charge, and nature of inhibitors [15]. As known that the benzimidazole is part of vitamin B12 and is a heterocyclic compound and is used in various fields such as dyes or pigments, optical sensing, electrolyte for fuel cells, *etc.* [16]. Moreover, the recent works reported benzimidazole and its derivatives can work as corrosion inhibitors due to the spatial molecular structure, surface charge density, electronic parameters, and their affinity for the metal surface [17]. A great deal of this work is synthesis a new corrosion inhibitor from benzimidazole. The benefits of this new derivative it can prepared at low cost and in one pot reaction, as well as the design of the synthesized compound was made from donor parts from benzimidazole and thiophene which is a rich in electrons with fully conjugated compound as well as the compound has three parts of resonance (two imidazole and thiophene). The structure of the studied inhibitor is approaching in Scheme 1. Another goal of this work is to investigate the effect of the SJ1 on the corrosion behavior of carbon steel in 0.1 hydrochloride acid by using different methods namely Tafel extrapolation technique, density Functional theory and supported by the investigated the surface morphology by using Atomic Force Microscope (AFM) and Scanning Electron Microscopy (SEM), respectively.

EXPERIMENTAL

Materials and Synthesis of SJ1 Inhibitor

In this work, all the starting compounds and solvents that have been used in the synthesis of the inhibitor SJ1 and the corrosive medium were of reagent grade and purchased from Sigma-Aldrich, and were used without further purification. To elucidate the chemical structure of the inhibitor under study was characterized by using several techniques; UV-Vis was performed by UV-1601(USA), the ^1H NMR and ^{13}C NMR were recorded on a 500 MHz Bruker-Plus (USA) spectrometer (Bruker, Germany) in

DMSO using TMS as a reference, the element analysis CHN was done by Carlo Erba 5500 elemental analysis, and the mass spectroscopy was recorded by Agilent 5973 (USA).

SJ1 was synthesized by refluxed ethanolic solution of 1*H*-benzo[*d*]imidazol-2-amine (1) (5.33×10^{-3} mmol, 0.712 g) and thiophene-2,5-dicarbaldehyde (2) (1.78×10^{-3} mmol, 0.25 g) and stirring for 18 h. The thin layer chromatography technique was used to monitor the completion reaction. The reaction mixture was cooled then filtered and washed with ethanol. Afterward, the product was dried and recrystallized by ethanol: acetone, (1:3), to yield 70.79% of solid red-purple compound with melting point of (197-200 °C) and the λ_{\max} was 430 nm in THF 1×10^{-4} M. The chemical structure of SJ1 was demonstrated in Scheme 1.

(*N,N'E,N,N'E*)-*N,N'*-(thiophene-2,5-diylbis(methanylylidene))bis(1*H*-benzo[*d*]imidazol-2-amine) (SJ1), $C_{20}H_{14}N_6S$, m. p.: 197-200 °C; 1H NMR (400 MHz, DMSO) δ 12.81 (s, 2H), 8.01 (s, 2H), 7.51 (s, 2H), 7.18-6.92 (m, 8H). ^{13}C NMR (100 MHz, DMSO) δ 158.26, 155.71, 155.35, 146.41, 137.51, 122.71, 119.39, 111.91, 56.48, 19.01. Anal. Calcd.; C, 64.85; H, 3.81; N, 22.69; Found C, 64.91; H, 3.77; N, 22.65; EI-MS: *m/z* 371.1.

Corrosion Test

The carbon steel specimens used in this study as working electrodes were supplied by one of the Metal Sample Companies, with the composition that given in Table 1. The corrosive medium 0.1 M hydrochloric acid solution was prepared from the analytical grade 37% HCl (Sigma Aldrich) by dilution with double-distilled water. Through this work, all carbon steel specimens were used within dimensions of (25 mm diameter and 3 mm height), but practically the carbon steel specimen effective area was 1 cm². Before each run, the surface of specimens was mechanically polished with fine grade emery paper (80/3000 grades), then washed with double distilled water, degreased with acetone, dried, and kept in a desiccator.

Electrochemical measurements were performed with a potentiostat (WENKING M Lab Bank Elektronik-Intelligent controls GmbH). M Lab is a multichannel potentiostat /galvanostat organized on a hardware board connecting to a computer by RS 232 cable. M Lab has three operation modes for each channel: (I) Potentiostatic mode (II) Galvanostatic mode (III) Open circuit mode. However, potentiodynamic polarization was conducted in a water jacketed three-electrode glass cell, and the three-electrodes corrosion cell is included; the carbon steel specimens as working electrode, platinum electrode, and silver-silver chloride electrode as a counter electrode and reference electrode, respectively. The specimens of carbon steel were immersed in the tested solution once in the absence of inhibitor and then in the presence of different inhibitor concentrations (0.1, 0.3, 0.5) mM with a range of temperature (293-323) K. The Tafel polarization measurement was made for a potential range (± 200) mV to the open circuit potential (OCP). All experiments for polarization curves were initiated about 30 min after the working electrode was immersed in the solution to stabilize the steady state potential. To confirm the reproducibility of the experiments, have been repeated the measurements three times, and only the average values are stated.

All corrosion parameters included the corrosion potential (E_c), and corrosion current density (i_{corr}) values were determined. Also, both Tafel slopes ' b_a ' and ' b_c ' are obtained from the slope of the linear Tafel portion of the anodic and cathodic curves, respectively [18]. From the polarization study, the inhibition efficiency (*IE*) was calculated by using Eq. (1) [19].

$$\%IE = \frac{i_{\text{corr}} - i_{\text{corr},i}}{i_{\text{corr}}} \times 100 \quad (1)$$

where i_{corr} and $i_{\text{corr},i}$ are the corrosion current densities without and with the presence of SJ1, respectively.

Surface Morphology Observation and Analysis

The surface morphology of carbon steel surface was

Table 1. Chemical Composition of the Carbon Steel Specimens Materials Used

Element	C	Si	Mn	S	P	Cu	Ni	Cr	Fe
%	0.42	0.30	1.40	0.05	0.05	0.50	0.20	0.20	96.88

also investigated in the absence and presence of corrosion inhibitor using Atomic force microscopy (AFM) which performance with the (AA3000\220V Angstrom, USA) and Scanning electron microscopy (SEM) (FEI Inspect-S50, Netherlands) techniques, respectively.

Computational Study

In order to reveal the optimization molecular structure of the synthesis inhibitor, as well as the mechanism of the inhibition, was carried out theoretically by using Density Functional Theory (DFT). The runs of Density functional theory (DFT) were carried out using the B3LYP functional at basis set of standard double-zeta plus polarization 6-311G(d,p) [20] implemented in the GAUSSIAN 09 software, and following the standard nomenclature, the calculation will be referred to as B3LYP/6-311G**. Quantum chemical parameters such as E_{HOMO} (highest occupied molecular orbital energy), E_{LUMO} (lowest unoccupied molecular orbital energy) and μ (dipole moment), (A) electron affinity, (I) ionization potential, (η) global hardness, (S) chemical softness, (χ) electronegativity and (ω) Electrophilicity Index were calculated, reported and discussed as shown in Eqs. ((2)-(8)) [20].

$$\Delta E = E_{LUMO} - E_{HOMO} \quad (2)$$

$$I(\text{Ionization potential}) = -E_{HOMO} \quad (3)$$

$$A(\text{Electron affinity}) = -E_{LUMO} \quad (4)$$

$$X(\text{Electronegativity}) = \frac{I + A}{2} \quad (5)$$

$$\eta(\text{Absolut hardness}) = \frac{I - A}{2} \quad (6)$$

$$S(\text{Chemical softness}) = \frac{1}{\eta} \quad (7)$$

$$(\text{Electrophilicity index}) = \frac{\mu}{2\eta} \quad (8)$$

RESULTS AND DISCUSSION

Synthesis of Inhibitor

New organic compound has been designed and

synthesized as a donor compound, which is fully conjugated, contained two aromatic rings (imidazole and thiophene) and has two types of heteroatoms (N and S). The compound was prepared in a simple Schiff base reaction by reacting one equivalent of thioaldehyde with two equivalent of imidazole derivative in ethanolic solution under reflux condition. The ^1H NMR and ^{13}C NMR were used to characterize the inhibitor. The ^1H NMR showed singlet peak, 2H, 8.01 ppm for N=CH (Schiff base) and multiple peaks from 7.18-6.92 for proton benzene rings. The ^{13}C NMR for SJ1 was showed the important peak at 158.26 ppm for Schiff base bond.

Potentiodynamic Polarization

Figures 1a-d shows the polarization curves for the carbon steel sample immersed in the corrosion medium in the absence and with the presences of different concentrations of SJ1 at four different temperatures (293, 303, 313, 323) K.

From Figs. 1a-d, it is obvious there is a difference in the Tafel region of the polarization curves and have found a linear relationship between the potential and the logarithm form of the current density. All the electrochemical kinetic parameters for corrosion process such as corrosion potential (E_{corr}), corrosion current density (I_{corr}), both cathodic and anodic Tafel slopes (b_c , b_a) were obtained by extrapolation of anodic and cathodic regions of the Tafel lines are listed in Table 2.

It can be seen from Table 2 that the polarization results showed that SJ1 had an impact effect on corrosion process if compared with the blank solution only, in general, the corrosion current density (which is directly proportioned with the corrosion rate) of the sample was decreased significantly after addition of SJ1, for example, at 293 in blank solution and with the presence of 0.5 mM SJ1, it is reduced from 139.99 $\mu\text{A cm}^{-2}$ to 7.87 $\mu\text{A cm}^{-2}$. in other words, the corrosion rate (C_R) is decreased with increasing SJ1 concentration and reduced from 14.38 to 0.808 mm/y, this is due to the phenomenon of the adsorption that can occur on to the surface of metal [21]. At the same time, the corrosion rate was increased significantly with increasing the temperature in the absence and presence of various concentrations of SJ1. Furthermore, the inhibition efficiency as evident from the decrease in C_R values with an increase in

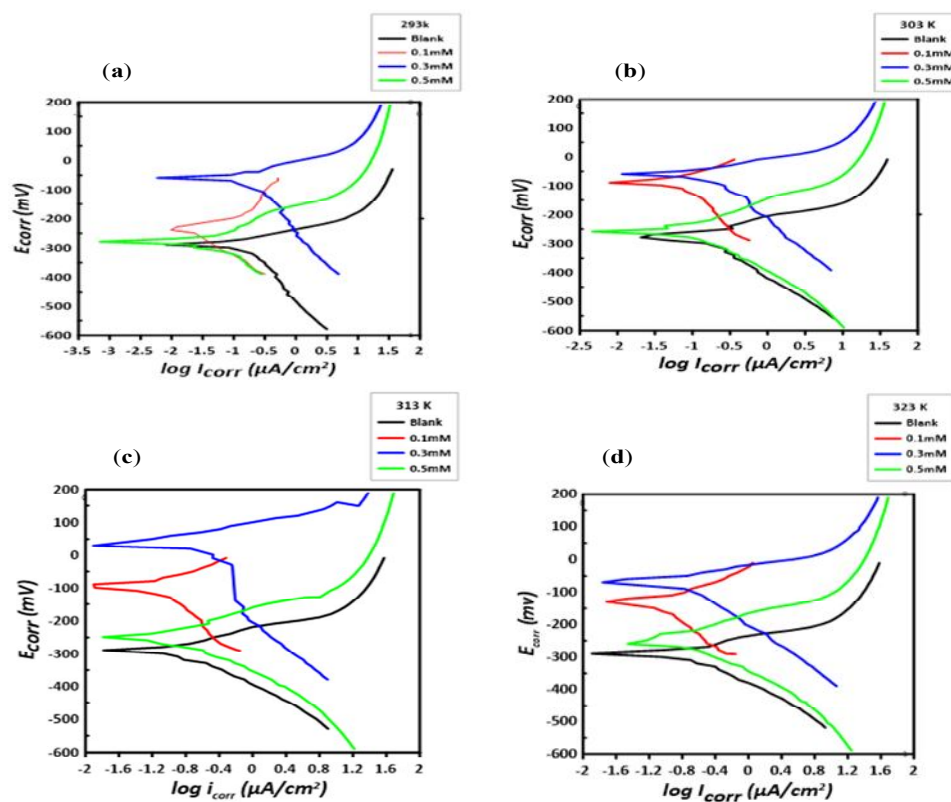


Fig. 1a-d. Polarization curves of carbon steel corrosion in the absence and presence of different SJ1 concentrations with a range of temperature (293-323) K.

Table 2. Corrosion Parameters Obtained From Tafel Scan for Carbon Steel in Absence and Presence of Different Concentrations of SJ1 at Range of Temperature (293-323) K

Conc. of SJ1 (mM)	Temp. (K)	$-E_{corr}$ (mV)	i_{corr} ($\mu\text{A cm}^{-2}$)	$-b_c$ (mV Dec $^{-1}$)	b_a (mV Dec $^{-1}$)	WL g/(m 2 *d)	C_R mm/y	θ	IE (%)
None	293	138.5	139.99	145.9	101.9	34.9	14.38	-	-
	303	141.0	256.55	186.7	130.6	56.4	23.22	-	-
	313	143.2	355.91	233.8	161.1	89.0	36.56	-	-
	323	143.7	458.41	299.3	175.7	116.0	47.09	-	-
0.1	293	79.5	25.33	139.6	78.7	6.4	2.60	0.82	82%
	303	85.7	46.16	136.5	69.1	11.5	4.74	0.80	80%
	313	104.0	78.79	200.6	125.8	9.7	8.09	0.78	78%
	323	104.6	128.54	303.6	139.1	21.0	13.20	0.72	72%
0.3	293	58.7	17.14	36.4	23.5	4.3	1.76	0.88	88%
	303	60.2	36.87	56.1	38.3	9.2	3.79	0.83	83%
	313	68.7	72.53	73.0	40.0	18.2	7.45	0.80	80%
	323	93.7	94.84	90.0	46.0	23.7	9.74	0.79	79%
0.5	293	277.5	7.87	40.7	30.6	1.8	0.81	0.96	96%
	303	280.3	15.65	45.4	47.3	3.9	1.61	0.93	93%
	313	281.2	33.68	56.1	51.0	8.4	3.46	0.91	91%
	323	281.9	53.99	59.3	49.4	0.6	5.546	0.88	88%

SJ1 concentration. However, SJ1 is considered as good inhibitor, if compared to the previous work that the highest $IE\%$ using different imidazole derivatives was between (60-70) [17,22], while in this work the highest $IE\%$ of 96.00% was observed at 293 K with using 0.5 mM SJ1. On one hand, Table 2 shown there is an appreciable improvement in the $IE\%$ from 82.00 to 96.00%, with increasing the inhibitor concentrations under the same experiment temperature. On the other hand, independent of the impact of SJ1 concentration, the corrosion of carbon steel was more and faster with an increase in experiment temperature. However, at each temperature, the effectiveness of SJ1 and its inhibitive action was predicted from the significant decrease in C_R and from the improvement increasing of the $IE\%$. From the results in Table 2, it can be realized that SJ1 could be adsorbed onto the carbon steel surface and provided a physical barrier to the corrosion media to interact with the surface of carbon steel, and this is also supported from the direct relation of SJ1 concentration and $IE\%$. On the other hand, with the further increase in solution temperature, the $IE\%$ was decreased from 96 to 88% and similar behavior at each addition of inhibitor concentration. This can be associated with the degradation and incompatibility of SJ1 with the surface of carbon steel at higher temperature, which also indicates that the action of SJ1 as inhibitor was hampered due to the increase of ionic mobility at the metal/electrolyte interface.

Moreover, Each additional of inhibitor concentration can play an important role in determining the type of inhibitor, as we can see from the polarization curve that the addition of various concentrations of SJ1 acts on both Tafel regions, the anodic and cathodic branches, which indicates that both anodic metal dissolution and cathodic reduction reactions were inhibited. This can explain to the difference of E_{corr} value respect to the corrosion potential of blank solution [23-24]. According to the literatures [23-24], it is said if the difference in the value E_{corr} ($\Delta E_{corr} = E_{corr,without} - E_{corr,with}$) is higher than 85 mV, then the inhibitor can be classified as a cathodic or anodic inhibitor, but if it is lower than 85 mV, in this case, the inhibitor can be considered as an inhibitor mixture. In this study our results have shown that the addition of SJ1 has some types of inhibitors due to the differences in the values of E_{corr} . The difference in value E_{corr} higher than 85 mV occurs at add 0.5 mM of SJ1, while

it was lower than 85 mV found at concentration of 0.1 and 0.3 mM of SJ1, that means the addition of 0.1 and 0.3 mM of SJ1 confirms that the SJ1 acts as a mixed inhibitor and in both cases of using 0.1 and 0.3 mM the SJ1 was dominated the anodic side due to the shift of polarization curves towards the positive side and in this case, SJ1 is maybe formed a thin layer onto the surface of the steel [25-26]. While the addition of 0.5 mM of SJ1 acted as a cathodic inhibitor and this was supported by the polarization curves demonstrated in Fig. 1d when the corrosion potential (E_{corr}) shifted to the more negative values (cathodic) in the presence of inhibitor. On the other hand, Table 2 shows there is a variation in b_a which is can be explain the formation of an adsorbed barrier layer, which was controlled the dissolution of carbon steel in HCl solution. Also from the results in Table 2 its clearly show that an increasing in temperature from 293 to 323 K, lead to increase the b_a values, but overall, decreasing trend of i_{corr} was detected with an increase in SJ1 concentration as given in Table 2. This behavior demonstrated that the SJ1 could cover the surface by forming a protective layer on the carbon steel and considerably improved the corrosion resistance as evident from the decrease in C_R with an increase in SJ1 concentration.

Also, it's apparent that the values of polarization resistance (R_p) obtained from linear polarization (LPR) studies are listed in Table 3 shown that R_p regularly increases with increasing the concentration of SJ1 and reaches a maximum of $0.964 \Omega \text{ cm}^2$ with the addition of 0.5 mM SJ1, if compared with the blank solution, which was only $0.186 \Omega \text{ cm}^2$. This indicates that the presence of inhibitor suggests there is a non-conducting physical barrier is formed at metal electrolyte interface [27].

The adsorption behavior and the thermodynamic parameters at various temperatures were also determined and discussed in the below sections.

Adsorption Study and Surface Coverage

There are different ways that the inhibitor molecules can adsorb onto the metal/alloy surface and the main step to justify the process of inhibitor adsorption on the surface of metal based on calculated the inhibition efficiency. Hence, the significant decrease in the corrosion current density suggests the strong interaction between the adsorbed

Table 3. The Polarization Resistance and Equilibrium Exchange Current Density for Carbon Steel Corrosion in the Absence and Presence of Various SJ1 Concentrations at the Range of Temperature (293-323) K

Conc. of SJ1 (mM)	Temp. (k)	R_p ($\Omega \text{ cm}^2$)	i_0 (A cm^{-2})
None	293	0.186	0.1380
	303	0.147	0.177
	313	0.116	0.232
	323	0.105	0.265
0.1	293	0.863	0.0297
	303	0.432	0.0604
	313	0.426	0.063
	323	0.322	0.086
0.3	293	0.362	0.0709
	303	0.268	0.097
	313	0.154	0.175
	323	0.139	0.2
0.5	293	0.964	0.026
	303	0.643	0.04
	313	0.344	0.078
	323	0.217	0.128

inhibitor molecule on the surface of the metal and formed a thin protective layer [28-29]. This layer can be expressed as the surface coverage (θ), and it's calculated as in Eq. (9), and the results are listed in Table 2

$$\%IE = \theta \times 100\% \quad (9)$$

Illustrated data in Table 2 show the linear relation between the surface coverage (θ) and different SJ1 concentration, and this connection is more suitable to Langmuir adsorption isotherm [30] which can be used to describe the type of the adsorption process as physical or chemical adsorption. However, The Langmuir model is expressed as in the following equation:

$$\frac{C}{\theta} = \frac{1}{K_{ads}} + C \quad (10)$$

where K_{ads} is the equilibrium adsorption constant and C is the concentration of inhibitor that are used. Figure 2 shows

SJ1 Langmuir adsorption isotherm in a 0.1 M HCl solution. The linearity in the results at various concentrations with correction factor ($R^2 > 0.9$) evidences that inhibition effect of SJ1 as a result of its molecules adsorption onto the carbon steel surface. Additionally, the free adsorption energy (ΔG_{ads}) for the 0.1 M HCl containing different SJ1 concentrations at the temperature range from 293-323 K was calculated from The Langmuir model, using the following relation:

$$K_{ads} = \frac{1}{55.55} e^{\frac{-\Delta G_{ads}}{RT}} \quad (11)$$

The obtained results for both K_{ads} and ΔG_{ads} are listed in Table 4.

Generally, the adsorption process is classified as physisorption or chemisorption according to the values of adsorption free energy value, if ΔG_{ads} around -20 kJ mol^{-1} or lower, in this case, the adsorption is physisorption due to the electrostatic interaction between the inhibitor molecule and the metal surface, whereas, the change of G_{ads} around -40 kJ mol^{-1} or higher, then adsorption that occurs is chemisorption, and this typically correlated with the charge sharing, or charge transfer from the inhibitor molecules to the metal surface to form a co-ordinate type of bond

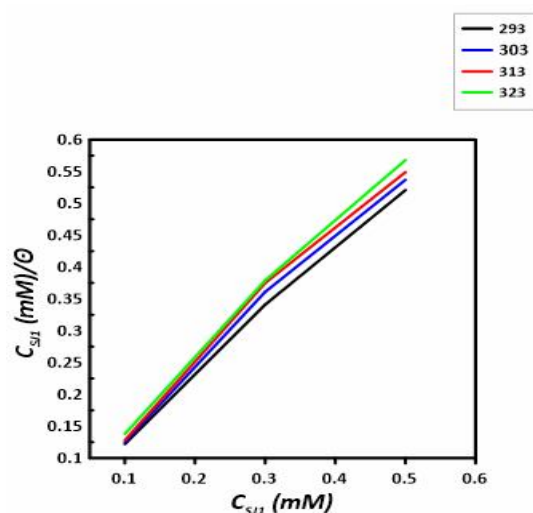
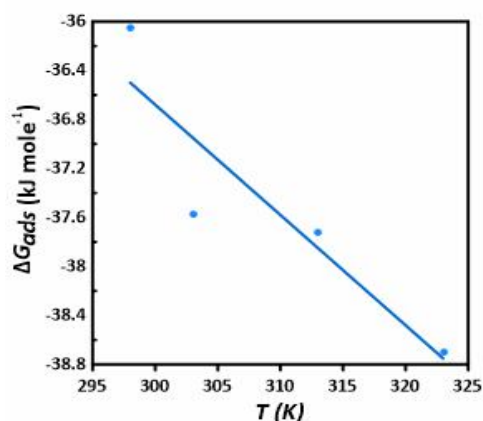
**Fig. 2.** Langmuir isotherm plot of SJ1 adsorption onto carbon steel surface in a 0.1 M HCl solution, at the range of temperatures (292-323) K.

Table 4. Thermodynamic Parameters of the Adsorption of SJ1 on Carbon Steel in 0.1 M HCl

Temp. (K)	K_{ads} (M^{-1})	$-\Delta G_{ads}$ ($kJ\ mol^{-1}$)	$-\Delta H_{ads}$ ($kJ\ mol^{-1}$)	ΔS_{ads} ($kJ\ K^{-1}\ mol^{-1}$)
293	36036.0	35.34	27.34	0.03
303	31250.0	35.00	26.72	
313	28639.2	34.78	26.23	
323	25531.9	34.50	25.68	

**Fig. 3.** Gibbs free energies (ΔG_{ads}) variation with temperature for SJ1 adsorption onto carbon steel surface in a 0.1 M HCl solution.

[31]. However, from the results in Table 4 it's obvious that the adsorption of SJ1 on the carbon steel surface is included both types of interactions with ΔG_{ads} of $-38.12\ kJ\ mol^{-1}$ with dominates chemisorption (mixed type adsorption). Furthermore, the negative value of ΔG_{ads} indicates that the adsorption process is spontaneous. The other thermodynamic parameters such as ΔH_{ads} and ΔS_{ads} are calculated from the Gibbs-Helmholtz equation, as shown below:

$$\Delta G_{ads} = \Delta H_{ads} + T\Delta S_{ads} \quad (12)$$

The plot of ΔG_{ads} against T for SJ1 adsorption on the carbon steel surface carbon surface in a 0.1 M HCL solution, over the temperature range from 293 K to 323 K, is shown in Fig. 3 and Table 4. From the results obtained as given in Table 4 the negative values of ΔH_{ads} means the adsorption

process is exothermic, this could explain why the Inhibition efficiency of adsorbed inhibitor molecules was decreased at higher temperature as seen in Table 2 [32]. Also, the inhibitor molecules adsorption is accompanied by ΔS_{ads} positive values, this is due to the disorder of the system as a result of adsorption of the inhibitor molecules onto the carbon steel surface.

Corrosion Kinetic

To further elucidate the influence of solution temperature on the inhibitive action of SJ1 on carbon steel surface was predictable from the Arrhenius equation [33], activation energy that is required for the progress of the corrosion process [34] was calculated from the following equation:

$$\log i_{corr} = \frac{-E_a}{2.303} RT + \log A \quad (13)$$

where A and E_a are the pre-exponential factor and the activation energy, respectively.

Figures 4a-b illustrates Arrhenius plots for the sample of carbon steel which was immersed in the blank and in the presence of different concentrations of inhibitor, values of E_a and A were derived from the slopes and intercept of the plots, respectively. The calculated values of E_a were higher for inhibited solutions to the blank solution which confirm the inhibitory effect of SJ1 on the corrosion process of the studied alloy [35].

Also, the values of standard enthalpy of activation (ΔH^*) and standard entropy of activation (ΔS^*) which can give some information about the formation of the activation, were calculated using the Arrhenius equation and its alternative formulation known as transition state equation were employed (14) [112].

$$i_{corr} = \left(\frac{RT}{Nh}\right) \exp\left(\frac{\Delta S^*}{R}\right) \exp\left(\frac{-\Delta H^*}{RT}\right) \quad (14)$$

where h is planks constant, N is Avogadro's number, T is the solution temperature, and ΔS^* and ΔH^* is the entropy of activation and is the enthalpy of the activation, respectively. However, Eq. (14) can be converted to:

$$\ln\left(\frac{i_{corr}}{T}\right) = \ln\left(\frac{R}{Nh}\right) + \left(\frac{\Delta S^*}{R}\right) - \left(\frac{\Delta H^*}{RT}\right) \quad (15)$$

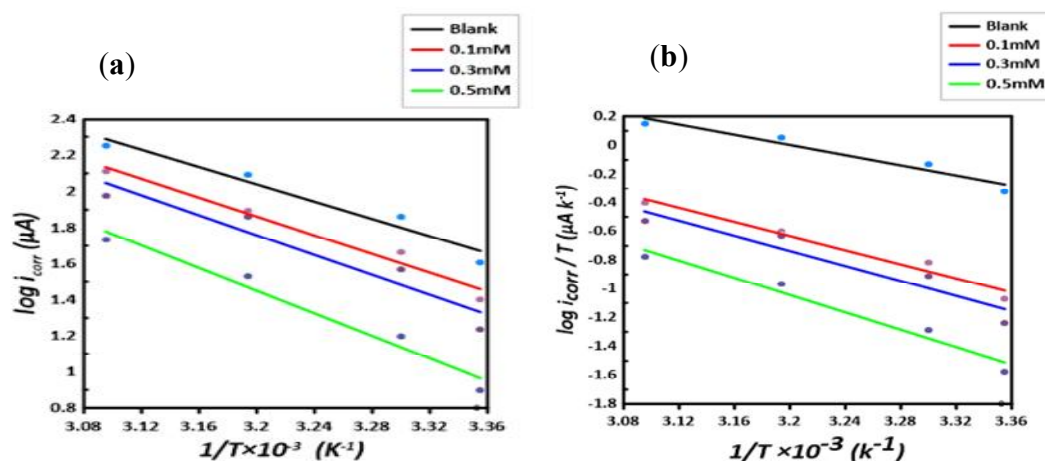


Fig. 4a-b. Arrhenius plots relationship for carbon steel corrosion in a 0.1 M HCl solution, in the absence and presence of various SJ1 concentrations at a range of temperature (293-323) K.

Table 5. The Activation Parameters for the Corrosion of the Carbon Steel Alloy in the Absence and Presence Various SJ1 Concentrations in the Temperature Range 293-323 K

Conc. of SJ1 (mM)	Temp. (K)	E_a (kJ mol ⁻¹)	A (dm ³ mol ⁻¹ s ⁻¹)	ΔH^* (kJ mol ⁻¹)	$-\Delta S^*$ (kJ mol ⁻¹ K ⁻¹)	ΔG^* (kJ mol ⁻¹)
None	293	36.81	0.5843×10^8	29.12	0.10	59.59
	303					60.63
	313					61.67
	323					62.71
0.1	293	42.58	9.954×10^8	40.03	0.08	63.82
	303					64.63
	313					65.44
	323					66.26
0.3	293	45.94	2.880×10^9	43.38	0.07	65.00
	303					65.32
	313					66.04
	323					66.77
0.5	293	51.57	1.242×10^{10}	49.02	0.06	66.65
	303					67.26
	313					67.86
	323					68.46

and ΔG^* can be calculated according to the following equation [33-34]:

$$\Delta G^* = \Delta H^* - T\Delta S^* \quad (16)$$

The values thus obtained, are recorded in Table 5, as seen from the results listed in the above Table 5 that the change

of ΔS^* for the sample test in the absence and presence of inhibitor is negative, this behavior could be mean that in the rate-determining step the activated complex is represented association rather than the dissociation step, and this lead to a decrease in disorder takes place [36]. It was also observed that the change of the activation enthalpy ΔH^* is positive for

blank solution and with the presence of different additive of SJ1, this behavior contributed to the endothermic property of the studied alloy, and this can be explained the negative effect of high temperature on the inhibition efficiency, which has been decreased with increasing the temperature [37].

Quantum Chemical Calculations

In order to examine the interaction nature between our new synthesis inhibitor (SJ1) and the studied alloy (carbon steel), DFT was performed to optimize the inhibitor structure and calculate the quantum chemical parameters such as highest occupied molecular orbitals (HOMO) and lowest unoccupied molecular orbitals (LUMO), which are reflecting the relation between the electronic structure of the

inhibitor molecule and its effect on the corrosion process. According to the Frontier molecular orbital theory, the reactivity of the molecule toward the adsorption on the metal surface is based on the tendency of donating and acceptance of electrons and this is related to the HOMO and LUMO values. Basically, the high value of HOMO (E_{HOMO}) refers to the higher donation ability of inhibitor molecule to the empty molecular orbital in the metal/alloy whereas, the low LUMO energy level (E_{LUMO}) refers to the ability of inhibitor to accept electrons [23-24,38-43]. Usually, the organic inhibitor can be as efficient corrosion inhibitors according to these two roles.

For SJ1, the calculated quantum chemical parameters are listed in Table 6 and the inhibitor optimized structure HOMO and LUMO are displaced in Figs. 5b, c, Fig. 5b

Table 6. Calculated Quantum Chemical Parameters of the Studied SJ1 Inhibitor, Using DFT Method

NO.	Parameters (eV)	Value
1	Energy of highest occupied molecular orbital (E_{HOMO})	-5.852
2	Energy of lowest unoccupied molecular orbital (E_{LUMO})	-3.124
3	Ionization potential (I)	5.852
4	Electron affinity (A)	3.124
5	Energy gap (ΔE)	2.73
6	Electronegativity (X)	4.488
7	Chemical hardness (η)	1.364
8	Chemical softness (σ)	0.733
9	Chemical potential (μ)	-4.488
10	Electrophilicity index (ω)	-7.383
11	Maximum charge transfer index (ΔN)	0.920
12	Dipole moment (Debye)	4.573

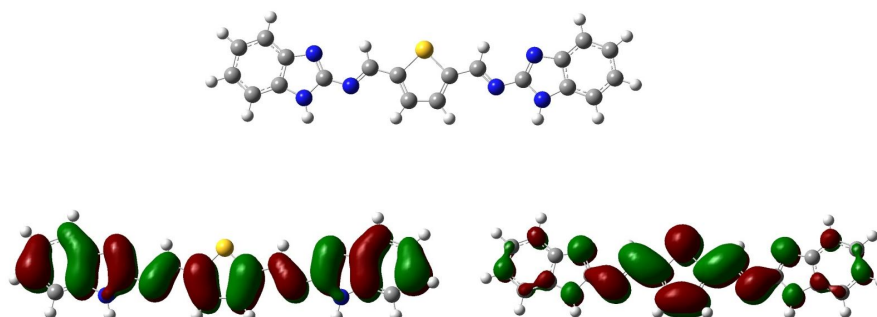


Fig. 5a-c. Molecular orbitals HOMO/LUMO for SJ1. (a) optimized structure of SJ1, (b) HOMO of SJ1, and (c) LUMO of SJ1.

shown that The electron distribution of HOMO was localized on the whole of molecules. This could be said that all parts of the inhibitor molecule can be considered as an adsorption active sites which will have the ability to donate the electrons to the empty (d-orbital) of Fe in the carbon steel and form a coordination bond. Furthermore, the presence of heteroatoms which are included S and N in the SJ1 structure, suggestion that the electrons may be mainly provided by these two atoms. Whereas the electron distribution of LUMO was mainly located in the center of the inhibitor molecule.

As well, the nature of strong or weak interaction that can be occurred between the active site of the metallic surface and inhibitor molecule is also based on the value of energy band gap ($\Delta E = E_{LUMO} - E_{HOMO}$) and the lower ΔE will lead to the strong interaction between the inhibitor and the surface of metal due to the formation of the protective film on the metal surface by adsorption of the inhibitor molecules [23-24].

On one hand, the other quantum chemical parameters that can give information about the relative reactivity or stability of a compound is the absolute hardness (η), which denotes the resistance ability of an atom to a charge transfer [44], and because the relation between the energy band gap and hardness this mean that the inhibitor molecule with lower hardness is more preferred as inhibitor because its ability to form the bond and anti-bond with the metallic surface through the donating or accepting electrons [45]. On the other hand, many studies show that (η) is not correlate and reflect the inhibition efficiency, this is due to the different adsorption mechanisms by using different materials [46-47]. Meanwhile, The inhibition efficiency of a compound can be explained by calculate the electronegativity (X) which is refer to the ability of an atom to attract electrons and retain its electrons via the donor-accepter interaction type then, this will lead to corrosion inhibition [48]. From Table 6 the lower values of electronegativity for SJ1 ($X = 4.488$ eV) and higher values of absolute hardness ($\eta = 1.364$ eV) if compared with Fe (metallic atom), mean the flow of electrons is occurring from the inhibitor molecule to the Fe atoms until the system reach and have the same chemical potential. Moreover, the fraction of electron transfer number (ΔN) has an impact on the inhibitive efficiency as well and is calculated as shown

in the following equation [49] :

$$\Delta N = (\chi_{Fe} - \chi_{MOTO}) / (2(\eta_{Fe} + \eta_{MOTO})) \quad (17)$$

where χ_{Fe} is the electronegativity of bulk iron was used (7 eV), η_{Fe} is the global hardness of iron (0). From the literatures it reported that if $\Delta N > 0$, this indicates there is an electron transfer from the inhibitor molecule to the metal surface and this [44-45]. In this work, the calculated ΔN for SJ1 is 0.920, which confirm that our new synthesis inhibitor SJ1 has an excellent ability to donate the electrons to the empty (d-orbital) of Fe and form a coordination bond and form adsorbed on to the surface formed a protective film layer which will reduce the metal corrosion. According to the HSAB theory, inhibitor molecule and metal can act as Lewis base and Lewis acid then will follow the principle of soft-soft and hard-hard. In this work, SJ1 can be considered as a soft base while Fe as soft acid, however, the high global softness values of SJ1 signify another evidence that it is an excellent corrosion inhibitor.

Mechanism of Corrosion Inhibition

Above all, and from the experimental values of thermodynamic parameters of adsorption process by using the electrochemical method it was clear that both types of interactions the physisorption and chemisorption are occurred in the adsorption process of SJ1 on the surface of carbon steel, with dominant of chemisorption and this supported by applied the method of quantum chemical calculations that based on used DFT method. This suggests that the chemisorption occurred due to the SJ1 molecules were adsorbed onto the carbon steel surface through formed the coordination bonds between the Fe atoms which are available on the surface of studied alloy and SJ1 molecules, and these bonds formed based on the donor-acceptor principle of electrons between the inhibitor molecule and Fe of carbon steel. The first and strongest possibility of coordination bonds formed is due to the electrons which are mainly donated from S or N atoms that presences in the SJ1 structure because these are heteroatoms and have a lone pair of electrons which is more easily to coordinate or transfer to the empty orbital (d-orbital) of Fe and form the coordination bond between the inhibitor molecules and the Fe, the second

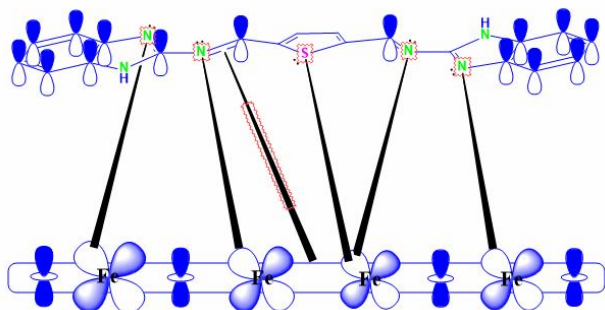


Fig. 6. Proposed mechanism of the SJ1 as corrosion inhibitor on Carbon steel.

possibility of coordination bonds formed is due to the π -electrons which available over whole the structure of inhibitor molecule as seen in Fig. 5b. The interaction between the d-orbital of Fe and the unshared and the π -electrons will lead to form the protective film layer over the surface of the alloy [35-37]. The planarity of SJ1 and due to the electron distributions over whole the molecule that indicated the SJ1 can adsorb onto the surface of carbon steel in parallel manner way as shown in Fig. 6.

Surface Morphology Studies

The surface morphology of the carbon steel samples in 0.1 M HCl in the absence and presence of 0.5mM of SJ1 is shown in Figs. 7a,b,c,d,e,f, by used both the AFM and SEM techniques, respectively. AFM technique was used to give information about the effect of SJ1 as an inhibitor on the corrosion of the alloy under investigation by study the morphology of the surface via measure the roughness of specimens that applied under the same conditions to study the surface morphology by using SEM. 2D and 3D AFM figures for the corroded and inhibited specimens are obtainable and displaced in Figs. 6a-d. The obtained results have shown that the average roughness of carbon steel surface in aggressive media is about (0.668 nm) as shown in Figs. 7a,b but it increased to (16.2 nm) by the addition of 0.5 mM of SJ1 at 323 as presented in Figs. 7c,d. This increase in average roughness of inhibited solutions is contributed to the aggregation of inhibitor molecules as cluster groups on the carbon steel surface [50-51].

Furthermore, to imagine the effect of the aggressive

medium on the surface of the carbon steel again in the absence and presence of 0.5 mM SJ1, SEM was recorded for the samples at 323 and presented in Figs. 8a,b. Figure 8a, shows the recorded image for the uninhibited surface of carbon steel in 0.1 M HCl, the bad damage on the surface is due to the corrosion process, while in the presence of inhibitor as seen in Fig. 8b it's shown that the molecules of the inhibitor adsorbed on the surface formed the protective film layer.

CONCLUSIONS

In conclusion, the easily prepared and costly effect of a new imidazole derivative (SJ1) was synthesized and characterized by using several spectrophotometric techniques and tested as an organic corrosion inhibitor for CS in the acidic medium by using both the experimental techniques and computational tools based on DFT. Obtained results from both experimental and theoretical analysis showed that the SJ1 can consider as an effective inhibitor for CS in 0.1 M HCl. The inhibition efficiency $IE\%$ was increased with increasing the SJ1 concentrations, but it decreased with rising the solution temperature and the maximum $IE\%$ was 96%. The analysis showed that the SJ1 can be adsorbed onto the CS surface, and its fit to the model of Langmuir adsorption isotherm, and have two types of interaction physisorption and chemisorption with predominated of chemisorption process. The obtained results from DFT calculations, which is included HOMO, LUMO, and band gap energy, shown that the SJ1 can donate the electrons from the whole inhibitor structure, but could be more easily from the heteroatoms that occur which are included (N and S) to the empty d-orbital of Fe in the CS forming coordinated bonds, which reflect the type of chemisorption. In addition, the Molecule planarity seems like another potential factor that reflects the capability of SJ1 to be a corrosion inhibitor via the strong adsorption capability onto the CS coupon tested. Overall, the analyses of the quantum chemical study based on the DFT calculations are in agreement with the experimental results. Also, the surface analysis by using AFM and SEM revealed that the addition of SJ1 to the aggressive medium in the maximum concentration (0.5 mM) at the highest tested

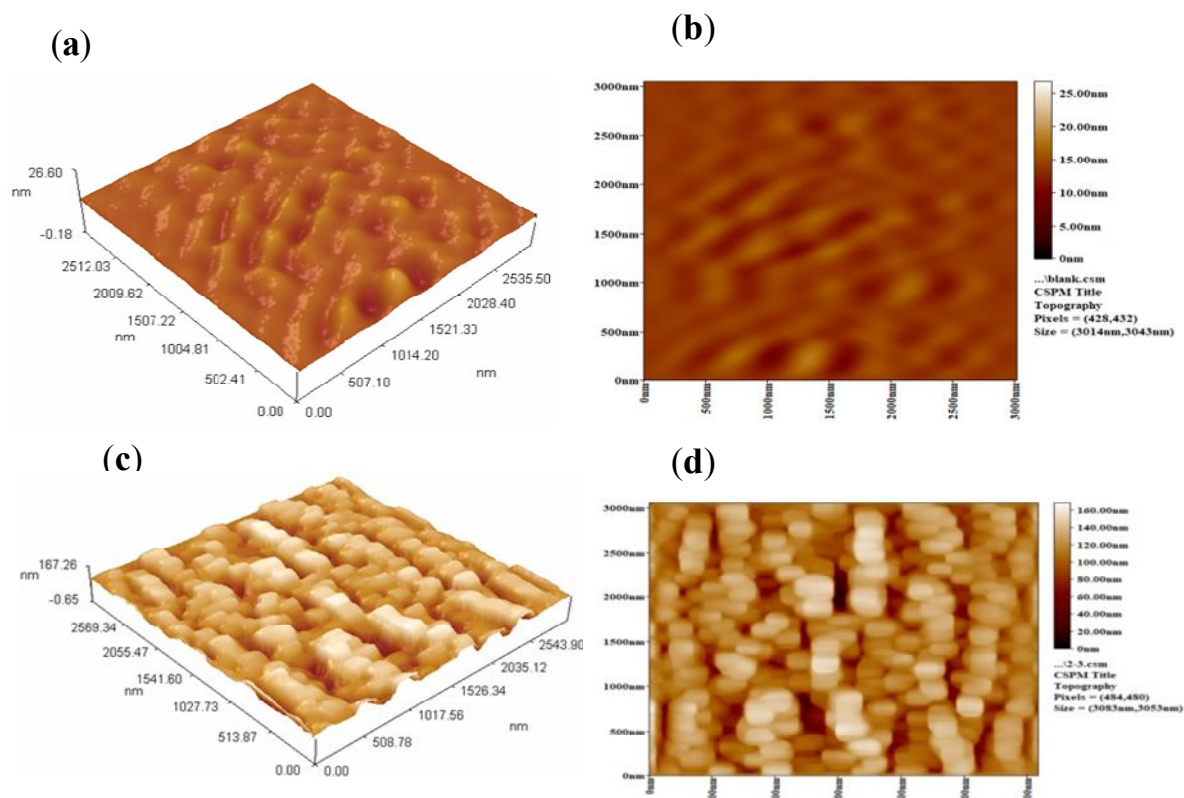


Fig. 7a-d. 3D and 2D AFM image of carbon steel in absence and presence of SJ1 inhibitor at 323K, (a-b) for corroded and (c-d) for inhibited.

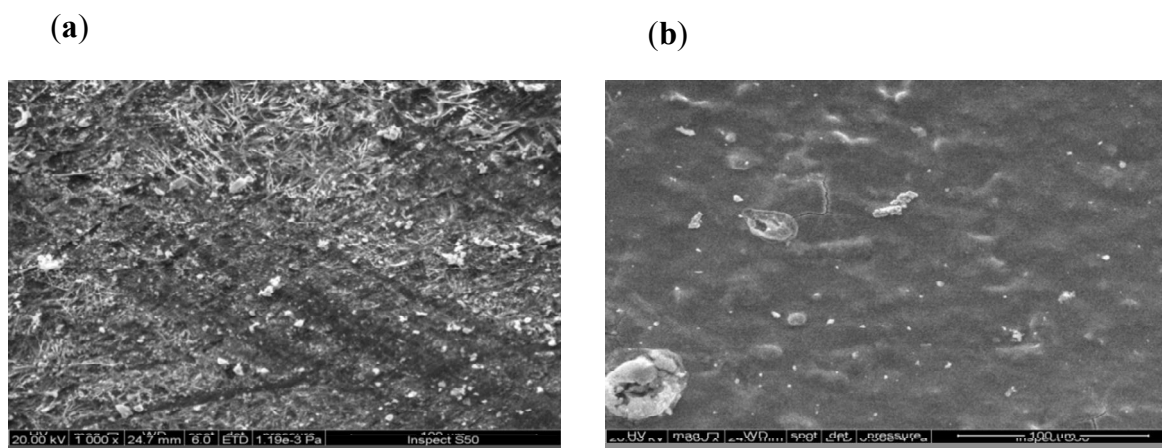


Fig. 8a-b. SEM for carbon steel in absence and presence of SJ1 inhibitor at 323K, (a) for corroded and (b) for inhibited.

temperature has an impact on controlling the corrosion of CS in 0.1 M HCl.

ACKNOWLEDGMENTS

Thanks go to Al-Nahrain university.

REFERENCES

- [1] Fouda, A. S.; Megahed, H. E.; Fouad, N.; Elbahrawi, N. M., Corrosion inhibition of carbon steel in 1 M hydrochloric acid solution by aqueous extract of thevetia peruviana. *J. Bio-Tribo-Corros.* **2016**, *2*, 16, DOI: 10.1007/s40735-016-0046-z.
- [2] Badr, G. E., The role of some thiosemicarbazide derivatives as corrosion inhibitors for C-Steel in acidic media. *Corros. Sci.* **2009**, *51*, 2529-2536, DOI: <https://doi.org/10.1016/j.corsci.2009.06.017>.
- [3] Dwivedi, D.; Lepková, K.; Becker, T., Carbon steel corrosion: A review of key surface properties and characterization methods. *RSC Adv.* **2017**, *7*, 4580-4610, DOI: 10.1039/C6RA25094G.
- [4] Aljourani, J.; Raeissi, K.; Golozar, M. A., Benzimidazole and its derivatives as corrosion inhibitors for mild steel in 1 M Hcl solution. *Corros. Sci.* **2009**, *51*, 1836-1843, DOI: <https://doi.org/10.1016/j.corsci.2009.05.011>.
- [5] Zhang, K.; Xu, B.; Yang, W.; Yin, X.; Liu, Y.; Chen, Y., Halogen-substituted imidazoline derivatives as corrosion inhibitors for mild steel in hydrochloric acid solution. *Corros. Sci.* **2015**, *90*, 284-295, DOI: <https://doi.org/10.1016/j.corsci.2014.10.032>.
- [6] Popoola, L. T.; Grema, A. S.; Latinwo, G. K.; Gutti, B.; Balogun, A. S., Corrosion problems during oil and gas production and its mitigation. *Int. J. Ind. Chem.* **2013**, *4*, 35, DOI: 10.1186/2228-5547-4-35.
- [7] Onyeachu, I. B.; Solomon, M. M.; Umoren, S. A.; Obot, I. B.; Sorour, A. A., Corrosion inhibition effect of a benzimidazole derivative on heat exchanger tubing materials during acid cleaning of multistage flash desalination plants. *Desalination* **2020**, *479*, 114283, DOI: <https://doi.org/10.1016/j.desal.2019.114283>.
- [8] Macedo, R. G. M. d. A.; Marques, N. d. N.; Tonholo, J.; Balaban, R. d. C., Water-soluble carboxymethylchitosan used as corrosion inhibitor for carbon steel in saline medium. *Carbohydr. Polym.* **2019**, *205*, 371-376, DOI: <https://doi.org/10.1016/j.carbpol.2018.10.081>.
- [9] Wei, W.; Geng, S.; Xie, D.; Wang, F., High temperature oxidation and corrosion behaviours of Ni-Fe-Cr alloys as inert anode for aluminum electrolysis. *Corros. Sci.* **2019**, *157*, 382-391, DOI: <https://doi.org/10.1016/j.corsci.2019.06.020>.
- [10] Ijaola, A. O.; Farayibi, P. K.; Asmatulu, E., Superhydrophobic coatings for steel pipeline protection in oil and gas industries: A comprehensive review. *J. Nat. Gas Sci. Eng.* **2020**, *83*, 103544, DOI: <https://doi.org/10.1016/j.jngse.2020.103544>.
- [11] Tiu, B. D. B.; Advincula, R. C., Polymeric corrosion inhibitors for the oil and gas industry: Design principles and mechanism. *React. Funct. Polym.* **2015**, *95*, 25-45, DOI: <https://doi.org/10.1016/j.reactfunctpolym.2015.08.006>.
- [12] Ansari, K. R.; Chauhan, D. S.; Singh, A.; Saji, V. S.; Quraishi, M. A., Corrosion Inhibitors for Acidizing Process in Oil and Gas Sectors. In *Corrosion Inhibitors in the Oil and Gas Industry*, **2020**, pp. 151-176.
- [13] Migahed, M. A.; El-Rabiei, M. M.; Nady, H.; Gomaa, H. M.; Zaki, E. G., Corrosion inhibition behavior of synthesized imidazolium ionic liquids for carbon steel in deep oil wells formation water. *J. Bio-Tribo-Corros.* **2017**, *3*, 22, DOI: 10.1007/s40735-017-0080-5.
- [14] El-Naggar, M. M., Corrosion inhibition of mild steel in acidic medium by some sulfa drugs compounds. *Corros. Sci.* **2007**, *49*, 2226-2236, DOI: <https://doi.org/10.1016/j.corsci.2006.10.039>.
- [15] Guo, L.; Obot, I. B.; Zheng, X.; Shen, X.; Qiang, Y.; Kaya, S.; Kaya, C., Theoretical insight into an empirical rule about organic corrosion inhibitors containing nitrogen, oxygen, and sulfur atoms. *Appl. Surf. Sci.* **2017**, *406*, 301-306, DOI: <https://doi.org/10.1016/j.apsusc.2017.02.134>.
- [16] Yadav, G.; Ganguly, S., Structure activity relationship (Sar) study of benzimidazole scaffold for different biological activities: A mini-review. *Eur. J. Med. Chem.* **2015**, *97*, 419-43, DOI: 10.1016/j.ejmech.2014.11.053.
- [17] Marinescu, M., Recent advances in the use of benzimidazoles as corrosion inhibitors. *BMC Chem.* **2019**, *13*, 136, DOI: 10.1186/s13065-019-0655-y.
- [18] McCafferty, E., Validation of corrosion rates measured by the tafel extrapolation method. *Corros. Sci.* **2005**, *47*, 3202-3215, DOI: <https://doi.org/10.1016/j.corsci.2005.05.046>.
- [19] Yang, W.; Wang, Q.; Xu, K.; Yin, Y.; Bao, H.; Li, X.; Niu, L.; Chen, S., Enhanced corrosion resistance of carbon steel in hydrochloric acid solution by eriototrya

- japonica thunb. Leaf eextract: Electrochemical study. *Mater. Lett.* **2017**, *10*, 956.
- [20] Nwankwo, H. U.; Olasunkanmi, L. O.; Ebenso, E. E., Experimental, quantum chemical and molecular dynamic simulations studies on the corrosion inhibition of mild steel by some carbazole derivatives. *Sci. Rep.* **2017**, *7*, 2436, DOI: 10.1038/s41598-017-02446-0.
- [21] Koumya, Y.; Idouhli, R.; Oukhrib, A.; Khadiri, M.; Abouelfida, A.; Benyaich, A., Synthesis, electrochemical, thermodynamic, and quantum chemical investigations of amino cadalene as a corrosion inhibitor for stainless steel type 321 in sulfuric acid 1 M. *Int. J. Electrochem.* **2020**, *2020*, 5620530, DOI: 10.1155/2020/5620530.
- [22] Garcia-Ochoa, E.; Guzmán-Jiménez, S. J.; Hernández, J. G.; Pandiyan, T.; Vásquez-Pérez, J. M.; Cruz-Borbolla, J., Benzimidazole ligands in the corrosion inhibition for carbon steel in acid medium: Dft study of its interaction on Fe₃₀ surface. *J. Mol. Struct.* **2016**, *1119*, 314-324, DOI: <https://doi.org/10.1016/j.molstruc.2016.04.057>.
- [23] Verma, D. K.; Ebenso, E. E.; Quraishi, M. A.; Verma, C., Gravimetric, electrochemical surface and density functional theory study of acetohydroxamic and benzohydroxamic acids as corrosion inhibitors for copper in 1 M HCl. *Results Phys.* **2019**, *13*, 102194, DOI: <https://doi.org/10.1016/j.rinp.2019.102194>.
- [24] Dagdag, O.; El Harfi, A.; Cherkaoui, O.; Safi, Z.; Wazzan, N.; Guo, L.; Akpan, E. D.; Verma, C.; Ebenso, E. E.; Jalgham, R. T. T., Rheological, electrochemical, surface, Dft and molecular dynamics simulation studies on the anticorrosive properties of new epoxy monomer compound for steel in 1 M HCl solution. *RSC Adv.* **2019**, *9*, 4454-4462, DOI: 10.1039/C8RA09446B.
- [25] Hussin, M. H.; Kassim, M. J., The corrosion inhibition and adsorption behavior of uncaria gambir extract on mild steel in 1 M HCl. *Mater. Chem. Phys.* **2011**, *125*, 461-468.
- [26] Pradityana, A.; Shahab, A.; Noerochim, L.; Susanti, D., Inhibition of corrosion of carbon steel in 3.5% Nacl solution by myrmecodia pendans extract. *Int. J. Corros.* **2016**, *2016*.
- [27] Banerjee, S.; Srivastava, V.; Singh, M. M., Chemically modified natural polysaccharide as green corrosion inhibitor for mild steel in acidic medium. *Corros. Sci.* **2012**, *59*, 35-41, DOI: <https://doi.org/10.1016/j.corsci.2012.02.009>.
- [28] Gerengi, H.; Sahin, H. I., Schinopsis lorentzii extract as a green corrosion inhibitor for low carbon steel in 1 M Hcl solution. *Ind. Eng. Chem. Res.* **2012**, *51*, 780-787, DOI: 10.1021/ie201776q.
- [29] Aljeboree, A. M.; Al-Baitai, A. Y.; Abdalhadi, S. M.; Alkaim, A. F., Investigation study of removing methyl violet dye from aqueous solutions using corn-cob as a source of activated carbon. *Egypt. J. Chem.* **2021**, *64*, 2873-2878, DOI: 10.21608/ejchem.2021.55274.3159.
- [30] Bobina, M.; Kellenberger, A.; Millet, J. -P.; Muntean, C.; Vaszilcsin, N., Corrosion resistance of carbon steel in weak acid solutions in the presence of L-histidine as corrosion inhibitor. *Corros. Sci.* **2013**, *69*, 389-395, DOI: <https://doi.org/10.1016/j.corsci.2012.12.020>.
- [31] Gupta, N. K.; Verma, C.; Quraishi, M. A.; Mukherjee, A. K., Schiff's bases derived from L-lysine and aromatic aldehydes as green corrosion inhibitors for mild steel: Experimental and Theoretical Studies. *J. Mol. Liq.* **2016**, *215*, 47-57, DOI: <https://doi.org/10.1016/j.molliq.2015.12.027>.
- [32] Benmahammed, I.; Douadi, T.; Issaadi, S.; Al-Noaimi, M.; Chafaa, S., Heterocyclic schiff bases as corrosion inhibitors for carbon steel in 1 M HCl solution: Hydrodynamic and synergetic effect. *J. Dispers. Sci. Technol.* **2020**, *41*, 1002-1021, DOI: 10.1080/01932691.2019.1614038.
- [33] Sliem, M. H.; Afifi, M.; Bahgat Radwan, A.; Fayyad, E. M.; Shibl, M. F.; Heakal, F. E.-T.; Abdullah, A. M., Aeo7 surfactant as an eco-friendly corrosion inhibitor for carbon steel in HCl solution. *Sci. Rep.* **2019**, *9*, 2319, DOI: 10.1038/s41598-018-37254-7.
- [34] Amin, M. A.; Ahmed, M. A.; Arida, H. A.; Arslan, T.; Saracoglu, M.; Kandemirli, F., Monitoring corrosion and corrosion control of iron in HCl by non-ionic surfactants of the triton-X series-Part Ii. Temperature effect, activation energies and thermodynamics of adsorption. *Corros. Sci.* **2011**, *53*, 540-548, DOI: <https://doi.org/10.1016/j.corsci.2010.09.019>.
- [35] Ahmed, S. K.; Ali, W. B.; Khadom, A. A., Synthesis and investigations of heterocyclic compounds as corrosion inhibitors for mild steel in hydrochloric acid. *Int. J. Ind. Chem.* **2019**, *10*, 159-173,

- DOI: 10.1007/s40090-019-0181-8.
- [36] Shreir, L. L.; Burstein, G. T.; Jarman, R. A., *Corrosion*, **1**, <http://www.sciencedirect.com/science/book/9780080523514>.
- [37] Singh, A. K.; Pandey, A. K.; Banerjee, P.; Saha, S. K.; Chugh, B.; Thakur, S.; Pani, B.; Chaubey, P.; Singh, G., Eco-friendly disposal of expired anti-tuberculosis drug isoniazid and its role in the protection of metal. *J. Environ. Chem. Eng.* **2019**, *7*, 102971, DOI: <https://doi.org/10.1016/j.jece.2019.102971>.
- [38] Abdalhadi, S. M.; Al-Baitai, A. Y.; Al-Zubaidi, H. A., Synthesis and characterization of 2,3-diaminomaleonitrile derivatives by one-pot schiff base reaction and their application in dye synthesized Solar cells. *Indones. J. Chem.* **2020**, *21*, 9, DOI: 10.22146/ijc.57535.
- [39] Jayaprakash, G. K.; Swamy, B. K.; Casillas, N.; Flores-Moreno, R., Analytical fukui and cyclic voltammetric studies on ferrocene modified carbon electrodes and effect of triton X-100 by immobilization method. *Electrochim. Acta.* **2017**, *258*, 1025-1034.
- [40] Jayaprakash, G. K.; Flores-Moreno, R., Quantum chemical study of triton X-100 modified graphene surface. *Electrochim. Acta.* **2017**, *248*, 225-231.
- [41] Jayaprakash, G. K.; Swamy, B. K.; Sánchez, J. P. M.; Li, X.; Sharma, S.; Lee, S.-L., Electrochemical and quantum chemical studies of cetylpyridinium bromide modified carbon electrode interface for sensor applications. *J. Mol. Liq.* **2020**, *315*, 113719.
- [42] Jayaprakash, G. K.; Swamy, B. K.; Rajendrachari, S.; Sharma, S.; Flores-Moreno, R., Dual descriptor analysis of cetylpyridinium modified carbon paste electrodes for ascorbic acid sensing applications. *J. Mol. Liq.* **2021**, *334*, 116348.
- [43] Jayaprakash, G. K.; Swamy, B. E. K.; Sharma, S.; Santoyo-Flores, J. J., Analyzing electron transfer properties of ferrocene in gasoline by cyclic voltammetry and theoretical methods. *Microchem. J.* **2020**, *158*, 105116.
- [44] Abd El-Lateef, H. M.; Tantawy, A. H., Synthesis and evaluation of novel series of schiff base cationic surfactants as corrosion Inhibitors for carbon steel in acidic/chloride media: Experimental and theoretical investigations. *RSC Adv.* **2016**, *6*, 8681-8700, DOI: 10.1039/C5RA21626E.
- [45] Parveen, M.; Mobin, M.; Zehra, S., Evaluation of L-tyrosine mixed with sodium dodecyl sulphate or cetyl pyridinium chloride as a corrosion inhibitor for mild steel in 1 M HCl: Experimental and theoretical studies. *RSC Adv.* **2016**, *6*, 61235-61248, DOI: 10.1039/C6RA10010D.
- [46] Verma, C.; Quraishi, M. A.; Olasunkanmi, L. O.; Ebenso, E. E., L-Proline-promoted synthesis of 2-amino-4-arylquinoline-3-carbonitriles as sustainable corrosion inhibitors for mild steel in 1 M Hcl: Experimental and computational studies. *RSC Adv.* **2015**, *5*, 85417-85430, DOI: 10.1039/C5RA16982H.
- [47] Gupta, R. K.; Malviya, M.; Verma, C.; Gupta, N. K.; Quraishi, M. A., Pyridine-Based functionalized graphene oxides as a new class of corrosion inhibitors for mild steel: An experimental and Dft approach. *RSC Adv.* **2017**, *7*, 39063-39074, DOI: 10.1039/C7RA05825J.
- [48] Verma, C.; Olasunkanmi, L. O.; Obot, I. B.; Ebenso, E. E.; Quraishi, M. A., 2,4-Diamino-5-(phenylthio)-5h-chromeno [2,3-B] pyridine-3-carbonitriles as green and effective corrosion inhibitors: Gravimetric, electrochemical, surface morphology and theoretical studies. *RSC Adv.* **2016**, *6*, 53933-53948, DOI: 10.1039/C6RA04900A.
- [49] Saha, S. K.; Ghosh, P.; Hens, A.; Murmu, N. C.; Banerjee, P., Density functional theory and molecular dynamics simulation study on corrosion inhibition performance of mild steel by mercapto-quinoline schiff base corrosion inhibitor. *Physica E Low Dimens. Syst. Nanostruct.* **2015**, *66*, 332-341, DOI: <https://doi.org/10.1016/j.physe.2014.10.035>.
- [50] Yaqo, E. A.; Anae, R. A.; Abdulmajeed, M. H.; Tomi, I. H. R.; Kadhim, M. M., Electrochemical, morphological and theoretical studies of an oxadiazole derivative as an anti-corrosive agent for kerosene reservoirs in iraqi refineries. *Chem. Pap.* **2020**, *74*, 1739-1757, DOI: 10.1007/s11696-019-01022-2.
- [51] Arshadi, M. R.; Lashgari, M.; Parsafar, G. A., Cluster approach to corrosion inhibition problems: Interaction studies. *Mater. Chem. Phys.* **2004**, *86*, 311-314, DOI: <https://doi.org/10.1016/j.matchemphys.2004.03.028>.